Integrated Master's in Biological Engineering

Master's thesis

Implementation of hiPSC-ECs in thrombosis-on-a-chip devices

João Pedro da Silva Simão

Instituto Superior Técnico, Lisbon, Portugal

Correspondence: silvasimao@tecnico.ulisboa.pt

Thrombosis, characterized by the undesired formation of blood clots within blood vessels, is one of the most important human vascular diseases and remains a major worldwide cause of myocardial infarction and stroke. However, its multifactorial nature and physiological and genetic-related variability makes research more difficult, and classical animal and *in vitro* models fail to accurately recapitulate *in vivo* human thrombogenesis. Rapid advancements in the field of microfluidics have recently brought promising results to this area of research, with devices of growing complexity and simpler processes of fabrication being developed. In parallel, the growth of human induced pluripotent stem cells (hiPSC) technology has also been predicted as a major step in scientific research and drug testing, representing a limitless source of human cells with patient-specific properties. Here, we aim at combining microfluidics with hiPSC technology to create patient-specific thrombosis-on-a-chip devices which can be used in research on the disease. Implementation of hiPSC-derived endothelial cells (hiPSC-EC) in the microchip was achieved and optimized and comparison between hiPSC-EC and human primary cells (HUVEC) displayed a more elongated, arterial-like morphology of the former. HiPSC-ECs were also hypothesised to have more plastic shear responsiveness than HUVECs, after nuclear alignment was observed when flow was present in the channel. During blood perfusion experiments in the microfluidic channels, hiPSC-EC presented characteristics similar to those of human primary cells (HUVECs), with comparable response to the inflammatory agent Tumour Necrosis Factor-α and reproduction of *in* vivo haemostatic mechanisms of platelet aggregation and fibrin deposition.

Keywords: Thrombosis-on-a-chip, Human induced pluripotent stem cells (hiPSC), Human Umbilical Vein Endothelial Cells (HUVEC), Microfluidics, Blood perfusion, Endothelium

Introduction

Thrombosis is an acute, severe condition affecting the vascular systems of thousands of people worldwide[1]. The disease is characterized by the undesired formation of a blood clot within a blood vessel and can lead to fatal cardiac arrest and stroke, remaining one of the most threatening but still inefficiently targeted pathologies known[2]. Most literature on thrombosis is either based on studies with animal models, which show distinct features from humans' systems and whose use in scientific studies carry several ethical issues, or inaccurate *in vitro* techniques, which are still not able to fully mimic complex conditions within human blood vessels and realistically address the disease[3,4].

However, recent advances in the fields of microfluidics and stem cells' technology promise to shed new light on the complex mechanisms of thrombogenesis and to take an important step towards thrombosis treatment. As more innovative protocols and techniques for microfabrication and microchips' designing are developed, more reliable become the artificial *in vitro* structures and conditions created to mimic natural human microenvironments. Already developed microchips with microchannels mimicking both healthy and injured, stenotic vessels[5,6] (characteristic of thrombotic situations), allow real time visualization of the distinct stages of thrombogenesis and therefore further our understanding of vascular pathologies.

As one of the main cellular components of the vascular system, the implementation of endothelial cells in microchannels to use on research is pivotal to study blood vessels and their intricate interactions *in vitro*. The use of standardized cell lines, such as human umbilical vein endothelial cells (HUVEC), is the most common approach in research, mainly due to their price, availability and practical methods of isolation[7]. However, as generic cell lines, they do not exhibit the specific features and behaviour of each patient's cells, and much of the variability inherent to the already reported genetic component of thrombogenesis[6] cannot be considered in these studies. Thus, research undertaken with these cell lines, although useful and practical, will always be generic, and conclusions reached will not be accurately addressable (regarding treatment for specific patients). To overcome this issue, many authors have been predicting the implementation and the regulated, widespread use of human induced pluripotent stem cells-derived endothelial cells (hiPSC-EC) in microchips to be the next major breakthrough in this field[4,8]. The introduction of hiPSC-EC in these microdevices is expected to allow for patient-specific evaluation of the disease and its causes (including genetic factors) and mechanisms, improving diagnosis and drug targeting and testing[9].

Following that line of thought, this work aims at combining human induced pluripotent stem cells derived endothelial cells (hiPSC-EC) with thrombosis-on-a-chip devices (previously designed and developed at the BIOS Lab-on-a-Chip Group, University of Twente), with the ultimate goal of advancing towards patient-specific analysis of the disease and its treatment. More specifically, this study explores the possibility of implementing, maintaining and testing hiPSC-EC within the aforementioned device in conditions mimicking those of real human blood vessels, including human blood perfusion, and to compare their morphology and performance when exposed to the inflammatory factor Tumour Necrosis Factor-α (TNF-α, reported to promote thrombogenesis[10]) and arterial shear rate to those of HUVECs (presently used in the microchips).

Materials and Methods

Device fabrication and preparation

The microfluidic device had been previously designed in BIOS, University of Twente (UT), using specialized computer-aided design (CAD) software. The rectangular-shaped, straight channels were designed to be 1 cm long (length), with dimensions of 300 x 50 μm (width x height). A silicon master mold with the desired structures was fabricated by photolithography. The master wafer was used for moulding polydimethylsiloxane (PDMS) microchips with the designed patterns by soft-lithography techniques[11]. PDMS silicone elastomer base was mixed with curing agent (both SYLGARD™ 184, Dow Corning) in a ratio of 10:1 and mixed thoroughly. Once mixed, PDMS was degassed for at least two hours, before being carefully poured on top of the wafer, inside an aluminium-wrapped glass Petri dish.

The Petri dish was then introduced in the oven (Quincy Lab Inc. Model 10 Lab Oven) for at least 3 hours (usually overnight) at 60ºC, for PDMS crosslinking. Once ready, the PDMS structure and the mould were carefully separated, single microchips were cut with a scalpel and 1 mm wide circular holes were punched in the designed inlet and outlet locations of the microchannels with a generic hole puncher.

Glass coverslips (ThermoFisher) were cleaned with ethanol and isopropyl alcohol (isopropanol). The surfaces of the slides and of the PDMS microchips were treated with air plasma in a CUTE plasma chamber (Femto Science). Activation by plasma promotes activation of the glass and PDMS, which were then brought to contact, promoting a permanent bond between the two – creating the final microfluidic device.

Cell culture of HUVEC and hiPSC-EC

HUVECs (Lonza, Pooled donor) were cultured and grown in collagen type I-coated T-75 flasks (CELLCOAT®, Greiner Bio-One) in EGM-2 endothelial cell growth media (Cell Applications, Inc). HiPSC were reprogrammed from human skin fibroblasts and differentiated into EC lines following previously reported protocols[12] (hisPSC-ECs were kindly provided to BIOS by the Leiden University Medical Center). HiPSC-ECs were grown in 0.1% gelatin-coated T-75 flasks in Human Endothelial Cells Serum Free Medium (EC-SFM) supplemented with 1% platelet-poor plasma-derived serum (Hycultec), 30 ng/mL of VEGF (R&D Systems) and 20 ng/mL of fibroblast growth factor (FGF, Miltenyi Biotec).

Chip coating and cell seeding

For promoting cell attachment, microchannels were coated with a solution of 0.1 mg/mL of rat tail collagen type I (Corning) and incubated at 37 ºC for 30 minutes (BINDER incubator). HUVECs in the T-75 flasks were detached by trypsinisation with 0.05% Trypsin (from a 0.5% Trypsin-EDTA stock solution, Gibco Life Technologies). HiPSC-ECs were detached with TrypLE (Gibco). Cells were counted and then introduced in the inlet reservoir of the coated microfluidic channels at approximately 15 x 10^6 cells/mL. The chip was incubated at an inverted position for 30 minutes at 37 ºC, 5% CO_2 (for seeding of the top part of the channels) and then re-seeded and incubated in a straight position (for seeding of the bottom part of the channel). Pipette tips with fresh EGM-2 medium were introduced in the inlets after incubation and replaced after 5 hours.

Inducing vessel wall dysfunction

For inducing endothelial inflammation, selected seeded channels with full monolayers were exposed to a solution of 10 ng/mL of TNF-α (Sigma-Aldrich) in EGM-2 medium for 16 hours (overnight exposure). At the end of the exposure period, fresh medium was flowed through the channels and pipette tips with fresh medium were introduced in the inlet reservoirs.

Blood samples and perfusion experiments

Citrated whole blood from human donors was provided by the Experimental Centre for Technical Medicine (ECTM) of the UT and used within 5 h of blood drawing, to reduce blood degradation and avoid time-dependent platelet activation or malfunction[10].

Microfluidic chips were placed in a Petri dish under the microscope (Leica DM IRM). A BD Luer-Lok 3 mL syringe was connected to Tygon plastic tubing (VWR) with customized connectors and a customized L-shaped metal tip in the end. This equipment was flushed with washing buffer, a solution of HEPES (Buffer Solution (1M), Gibco), 1% glucose (Merck Millipore), 1% BSA (Sigma), 200 mM CaCl2 (Sigma) and 0.1 µ/mL heparin (Sigma), meant

to prevent the blockage of the tubing due to clotting. The syringe was placed in a syringe pump (Harvard Apparatus PHD 2000 Programmable) and the metal tip was introduced in the outlet of the target channel of the microchip. From this point on, lights were turned off to avoid photobleaching.

Labelled fibrinogen (Alexa647, Invitrogen) and CD41 labelled primary antibody (PE, Invitrogen) were directly added to the blood tube at 7 µl/mL and 10 µl/mL and incubated at room temperature (RT) for 10 minutes. A solution of MgCl2 (31.6 mM) and CaCl2 (63.2 mM) in HEPES, used as the recalcification buffer, was added at 1:10 (100 µl/mL) to the blood sample.

Recalcified blood was perfused at 7.5 µl/min (1000 s^{-1}, arterial shear rate[6]) through the channel. Real-time platelet aggregation was followed and recorded using the side camera and original software of the Leica microscope.

Labelling and microscopy

For observation and comparison of the morphologies of HUVECs and iPSC-ECs (both static and after blood perfusion), nuclear staining (NucBlue™ Live ReadyProbes, ThermoFisher Scientific) and VE-cadherin primary (rabbit polyclonal, Abcam) and anti-rabbit secondary (AlexaFluor 488, goat polyclonal, Abcam) antibodies were used.

Microchannels were washed with phosphate-buffered saline (PBS) solution and fixated with 4% formalhdehyde (from a 37% stock solution, Sigma) in PBS for 20 minutes at RT. Channels were re-flushed with PBS, flooded with a 1 µg/mL primary antibody in PBS with 1% bovine serum albumin (BSA, Sigma) and incubated overnight at 4 ºC. The channels were then washed with PBS and a 10 µg/mL secondary antibody solution was added (incubation for 1h at RT). Nuclear staining was added and left for 30 minutes at RT and channels were then re-flushed. Fluorescent staining was observed with an EVOS Fl microscopy system (Invitrogen).

In tests for platelet activation, VE-Cadherin primary antibody was replaced by P-Selectin labelled primary antibody (FITC, Santa Cruz) at 10 µg/mL in PBS with 1 % BSA. The rest of the protocol was followed as previously described.

Analysis of blood perfusion data - comparison between HUVECs and hiPSC-ECs

After blood perfusion, fixated and stained microchips were used to obtain endpoint measurements and data on platelet coverage and average clot size on healthy and injured HUVECs' and hiPSC-ECs' endothelial layers. Four fixed points of each channel used for blood perfusion (near the inlet, around 1/3 of the channel, around 2/3 of the channel and near the outlet) were chosen and pictures were taken (same points for all chips).

Data from the edges of each channel was discarded, to reduce the influence of edge-effects (only the middle 200 µm section was considered). Platelet coverage was estimated using the triangle script of the software Matlab 2016b and surface area of the clots was determined with the regionprops script. Statistical analysis of the results was performed using a T-test (Student's *t*-Test) with a significance level of 5%. This was made in Microsoft Excel software, using two distinct methods to confirm the results: the software's Data Analysis package and the direct Excel's function (t-test). For each healthy condition (HUVECs and iPSC-ECs), data from two independent experiments was considered. For each diseased condition (HUVECs and iPSC-EC exposed to TNF-α), three independent experiments were analysed.

Results and Discussion

Cell growth and on-chip implementation

HiPSC-ECs growing in the T-75 flasks showed endothelial-cell-like morphology (data not shown). However, it was noticeable that hiPSC-ECs presented a more elongated, spindle-shaped structure when comparing to the characteristic cobblestone morphology of HUVECs. This had already been described by Belt et al[13], who showed spindle-like morphology in hiPSC-ECs growing in T-75 cultures and reported a shift into a more fibroblast-like morphology after prolonged culture.

Several seeding densities for on-chip cultures were tested, with the goal of reaching an optimal value at which the channels with healthy, confluent monolayers of HUVECs and hiPSC-ECs could be used at the end of the same day they were seeded. Previously developed protocols[10,14] described the optimal seeding density of HUVECs in these devices to be between 5 x 10^6 cells/mL and 20 x 10^6 cells/mL. After about 5 of cell seeding, it was found that seeding densities below 10 x 10^6 cells/mL resulted, with few exceptions, in incomplete monolayers of attached cells (fig. 1A) which did not reproduce the epithelial layer of human blood vessels. On the other hand, seeding densities above 15 x 10^6 cells/mL (and bellow 20 x 10^6 cells/mL) mostly resulted in full monolayers of cells (both hiPSC-ECs and HUVECs), that could line the entire inner walls of the microchannels (fig. 1B). Yet, some of the channels with higher seeding densities (around 20 x 10^6 cells/mL) presented overconfluent layers with some cell death which could influence the result of the experiments. Thus, the seeding density deemed optimal for implementing hiPSC-ECs and HUVECs in the microfluidic devices in use was set to 15 x 10^6 cells/mL.

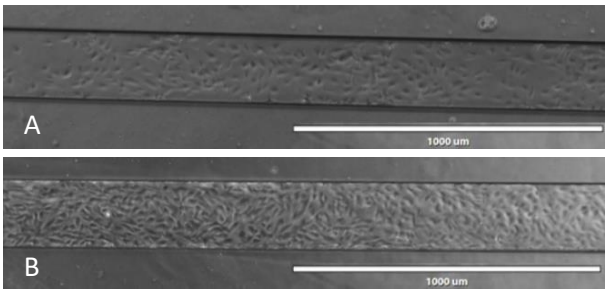

Figure 1 - Thrombosis-on-a-chip device's microchannels seeded with HUVECs. Pictures were taken 5 hours after cell seeding. In A, the channel was seeded at around 5 x 10^6 cells/mL; in B, it was seeded at around 20 x 10^6 cells.

Static on-chip morphology of hiPSC-ECs and comparison with HUVECs

Seeding with both cell types resulted in a full, apparently healthy monolayer of endothelial cells. However, differences in the organization of the monolayer and the orientation and morphology of individual cells were visible under microscopy, even with low magnification (fig. 2A and B).

The main noticeable distinct feature between the two channels was the general organization and orientation of the cells that formed each monolayer. It is possible to see that the hiPSC-ECs created an organized, similarly aligned layer of cells (fig. 2B and D). They also show an elongated shape, with similar nuclear alignment. In contrast, HUVECs show no alignment of nuclei or cytoskeleton and no changes to their cobblestone-like morphology (fig. 2A and C), presenting their normal structure for static environments. Since hiPSC-ECs were observed to have no special alignment during growth and even after reaching confluency in microwells[15] the depicted morphology was not to be expected, since no perfusion experiments were done, and no shear was being purposely applied.

Two hypotheses for the observations were drawn: either cells were simply adopting the most efficient shape and distribution inside the channel, or enough flow was being created during seeding and medium replacement to induce these phenotypic changes. The hypothesis that an exterior factor was responsible for the observed reorganization was supported by the fact that every hiPSC-EC in every

seeded microfluidic device was aligned and elongated in a close-to-horizontal angle, never vertically. This suggests that the observed phenotypic adaptation was not arbitrary and that it was likely related to the direction which the fluids were taking inside the channel (causing shear stress), even at low flow rates.

Different groups reported observation of phenotypic alterations, characterized by elongation and cell alignment, in hiPSC-EC under dynamic conditions[16,17]. Shear stress is known to influence arterial marker expression[18] in these cells, even at values as low as from 0.1 to 5 dyne/cm^2 (physiological shear stress of veins and venules[16]). Furthermore, when comparing the adopted morphology and alignment of hiPSC-EC, HUVECs and Human Umbilical Arterial Endothelial Cells (HUAECs) after 24h of perfusion at low, venous shear rate, Smith et al[17] reported that HUVECs failed to realign as consistently as the other two cell lines. Considering an approximate value for the dynamic viscosity of the medium of 7.5x10^{-3} dyne.s/(cm^2) and an estimated flow rate of 1.7 µl/min during medium replacement, from one pipette tip to the other (see in more detail in [5]), the shear stress would be of around 1.7 dyne/cm^2 (venous shear) in the thrombosis-on-a-chip microchannels during these periods, and higher during seeding and blood perfusion. Although for short periods of time, cells were exposed to these intermittent conditions (dynamic and static) for approximately 24h.

This is possibly the explanation for the alignment and elongation of hiPSC-ECs. The fact that HUVECs did not alter their morphology or alignment is also in accordance with Smith et al results[17]. Our morphology experiments support their conclusion that hiPSC-ECs have more plastic shear responsiveness than HUVECs. To note that hiPSC-ECs' response to shear stress in Smith's studies was closer to those of HUAECs, which also changed orientation and elongated under venous flow rate, than to those of HUVECs. This is suggestive of a more arterial-like nature of hiPSC-ECs, also reported by other authors in static experiments[16,19].

Under higher magnification, distinct features are observed with the VE-cadherin labelling. In fig 2C,

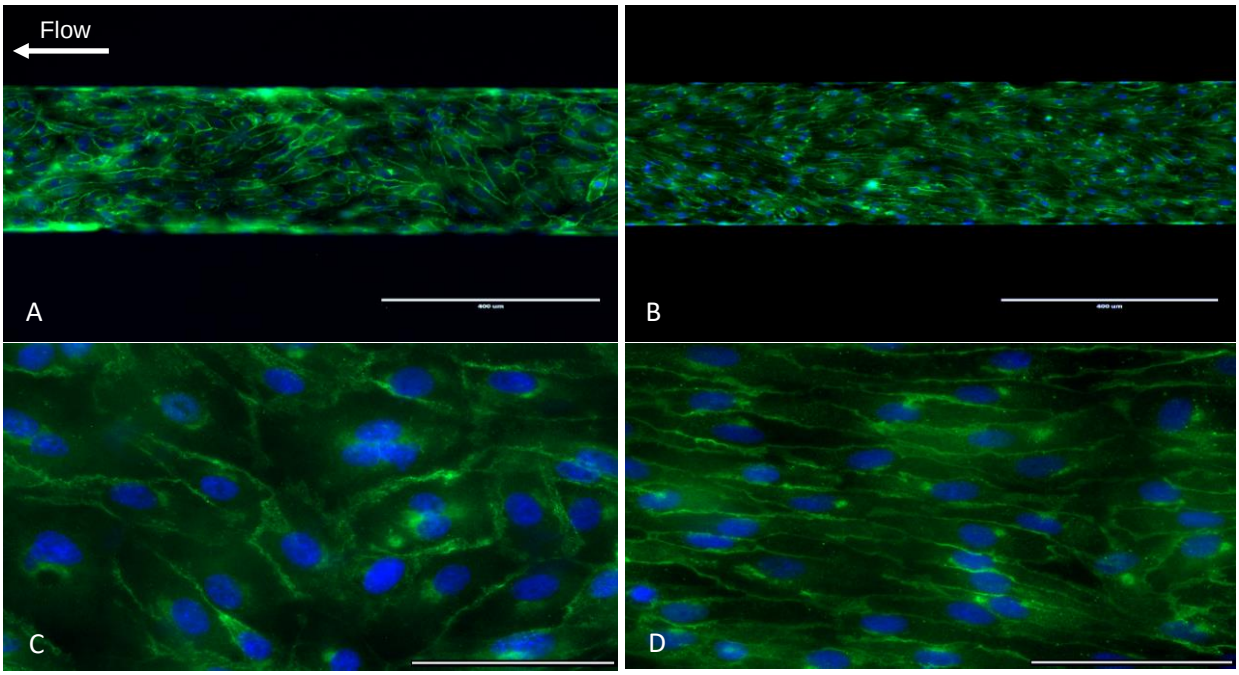

Figure 2 - Microchannels lined with healthy endothelia of HUVECs (A,C) or hiPSC-EC (B,D), with lower and higher magnification. Nuclei were stained with NucBlue, in blue (DAPI); adherens junctions with VE-cadherin antibody and AlexaFluor488 labelled secondary antibody, in green (GFP). Scale bars, 400 µm in A, B and 50 µm in C, D. Flow from right to left.

HUVECs present spread in-between cells staining, with blurred areas of VE-cadherin-stained structures. Conversely, hiPSC-ECs stained adherens junctions form thin, well-defined lines of cell-cell interactions (fig. 2D). These observations are in agreement with those of Halaydich et al[19], when culturing these cells lines in static conditions. In that study, the CD31+ hiPSC-EC line (the same of the present report) presented highly organized adherens junctions and tight junctions in junctional integrity assays, in contrast with HUVECs' apparently less organized and defined cell-cell connections.

Finally, and even though the two cell lines presented relevant morphological differences and distinct responsiveness to low shear stress, it was deemed that both adapted positively to the microchannels. Neither hiPSC-ECs nor HUVECs displayed visible signs of stress, showing full, healthy monolayers and intact cell-cell interactions.

Blood perfusion on-chip – clot formation and composition and platelet activation

The goal of blood perfusion experiments was not only to analyse hiPSC-ECs endothelium's ability to react to injury and recreate thrombotic events on-chip but also to confirm platelet activation and compare clots' composition to those described in *in vivo* and *in vitro* studies.

In fig. 3A, obtained in a TNF-α treated channel after blood perfusion, several points of platelet aggregation can be observed in the channel.

On the one hand, platelets adhering to gaps where no endothelial cells were seeded (clots identified in white) can be seen. Gaps in the monolayer were not to be expected and could either be related to the adaptation to the sudden change in shear stress, to the exposure to TNF-α or with some flaws in the monolayer originally formed during seeding (which may have been enhanced by shear stress and the inflammatory agent). However, confirming that platelets are adhering to exposed collagen was deemed of relevance, since it shows that platelets from the donors' blood are keeping their ability to interact with the extracellular matrix (ECM) proteins and aggregate on the *in vitro* exposed ECM layer, as it would happen after severe vessel injury.

On the other hand, it is also possible to observe zones of platelet aggregation on top of seeded endothelial cells (clots identified in orange, in fig. 3A). In fig. 3B, it can be observed that the signal corresponding do CD41-labeled platelets overlays and crosses the organized green lines corresponding to cell-cell connections between cells (identified through VE-cadherin), instead of gaps in the monolayer. This strongly suggests that cells are

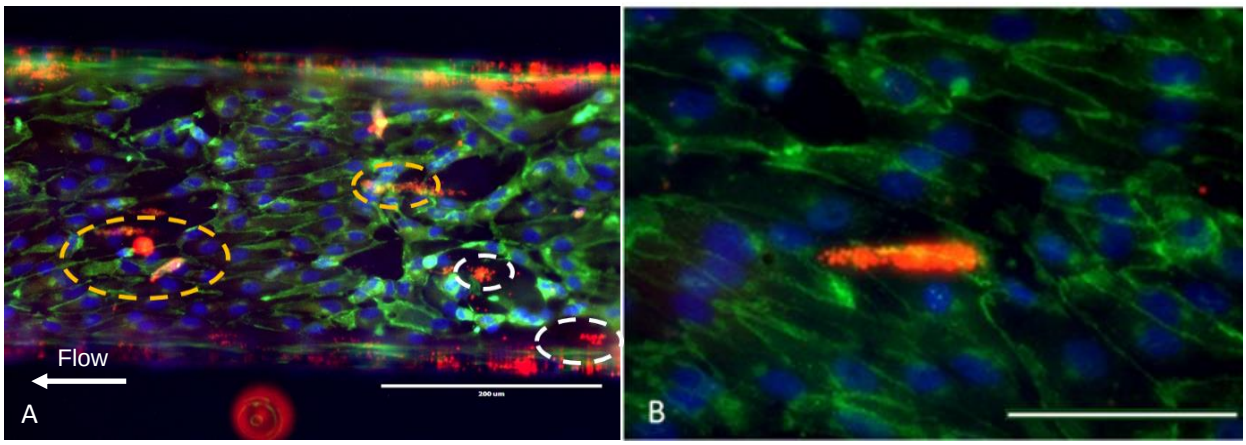

Figure 3 - Staining of a treated hiPSC-EC channel after blood perfusion (A) and clot formation (B). Nuclei stained in blue (DAPI), VE-cadherin in green (AlexaFluor 488, GFP) and platelets' CD41 in red (PE, RFP). Scale bar, 200 µm (A) and 50 µm (B).

becoming injured after exposure to the inflammatory agent and that it is possible to develop thrombosis-on-a-chip with hiPSC-ECs by inducing vessel wall dysfunction.

Furthermore, the teardrop-like morphology see in fig 3B had been reported in previous works with *in vitro*[10] and *in vivo*[20] blood perfusion and considered characteristic of the dynamic environment created in blood vessels. This observation supports the hypothesis that *in vivo* thrombosis-like events are being reproduced on-chip.

Another important marker of haemostatic mechanisms and thrombogenesis is platelet activation. P-Selectin was found to be present in several areas where platelets were aggregating (fig. 4), suggesting that a part of these were displaying their activated state. This observation is indicative that platelets circulating in the channel (whilst blood is being perfused) were able to display markers of activation when aggregating. Platelet activation is an essential stage of primary haemostasis[2,21] and thrombi formation in *in vivo* injury response.

Lastly, fibrin deposition was assessed during perfusion experiments. The growing clots were mainly composed of platelets and a supportive mesh of fibrin (fig. 5), reported characteristics of *in vivo* arterial blood clots[10,21]. The presence of a network of fibrin on and around the clot indicated that ECs in the microchannels were still able to promote the conversion of fibrinogen to fibrin, retaining their natural ability to trigger the coagulation cascade in response to injury[2,10]. This is a critical step of *in vivo* secondary haemostasis and, together with the demonstration of platelet activations, indicates that full haemostasis (primary and secondary) is taking place in the microfluidic device, an essential step towards realistic *in vitro* reproduction of thrombosis.

Comparison between hiPSC-EC and HUVECs' platelet coverage and average clot size

As expected, platelet coverage values on untreated, healthy channels were low, compared to the ones obtained for TNF-α treated endothelium (fig. 6). However, high variability was verified among sets from different days of blood perfusion experiments (as seen in data points of treated endothelium in fig. 6). This variability was considered to be mainly related to the intrinsic blood-variability. Blood and donor-variability are well-documented causes of unpredictability in blood perfusion experiments[14] and can lead to different responses of circulating cells and of the endothelium to the tested conditions.

After automated image analysis, average platelet coverage in untreated hiPSC-ECs and HUVECs channels were estimated as 0.4 % and 0.5 %,

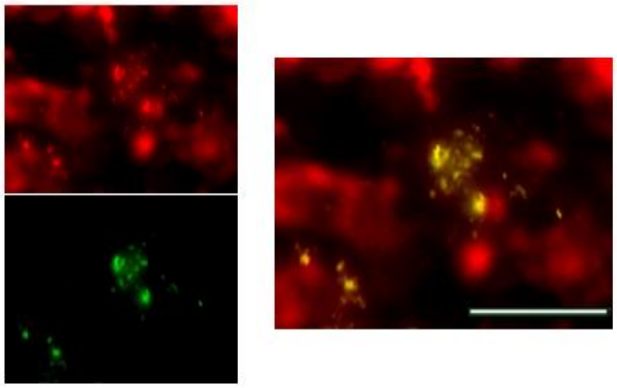

Figure 4 - Fluorescently labelled clots and activated platelets. RFP channel (CD41, image A) and GFP (P-Selectin) were merged together to confirm overlay (C). Scale bar, 50 µm

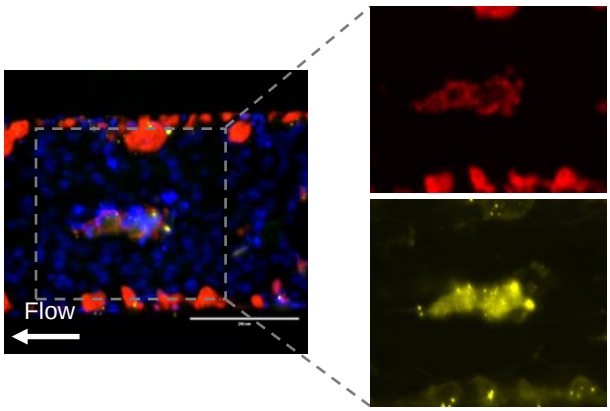

Figure 4 – Fluorescently labelled clots. RPF (CD41, B) and Cy5 (fibrin, C) channels were split from A for visualization of the clot composition. Scale bar, 200 µm.

respectively. Treated channels, however, showed 2.8 % and 3.1 % of average platelet coverage for hiPSC-ECs and HUVECs, respectively (fig. 6). These results suggested a difference between average platelet coverage of different cell lines existed and that the HUVECs inflamed endothelium demonstrated higher tendency for platelet attachment than the hiPSC-EC endothelial layer. Furthermore, a difference in average clot size was also verified: while hiPSC-EC presented clot sizes of 38 μm^2, HUVECs' were estimated as 44 μm^2. However, Student's t-test analysis of both sets suggested that there was no statistical significance in the difference in coverage between both cell lines (P-value=0.77 at a 0.05 significance level). Thus, the test failed to reject the original null hypothesis (that no difference existed between sets).

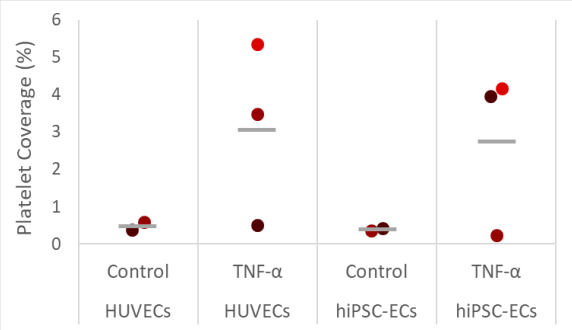

Figure 5 - Representation of the platelet coverage (%) in the experiments with treated and untreated HUVECs and hiPSC-ECs. Each point's colour represents a different day of experiments (n=2 for untreated and n=3 for treated endothelium). The mean values are represented by grey lines.

More repetitions of the present experiments must be made to reduce variability and before more precise and reliable conclusions regarding platelet coverage in both types of endothelium can be drawn. However, following reports of lower levels of vWF, lower expression levels of pro-inflammatory adhesive receptors and less leukocyte attachment in hiPSC-ECs than in HUVECs (in assays realized by Halaidych et al[19]), a difference in future thrombogenesis assays between both cell lines is expected (with an aggravated response of HUVECs to perfusion)

Conclusions and future work

In this work, successful implementation of an *in vitro* endothelium of hiPSC-ECs in thrombosis-on-a-chip devices was achieved. In contrast with HUVECs' cobblestone morphology, hiPSC-ECs displayed an elongated, spindle-like morphology in static and dynamic conditions, and observations of cell and nuclei alignment in the channel suggested high plastic responsiveness to shear.

A proof-of-concept experiment of human blood perfusion and *in vitro* thrombosis induction with hiPSC-ECs was also performed in the microchip. *In vivo*-like primary and secondary haemostatic mechanisms were triggered, since platelet activation and aggregation and fibrin deposition were observed in treated channels. During blood perfusion, HUVECs presented higher platelet coverage and larger clots than hiPSC-ECs. This is in line with recent findings that pointed at higher basal levels of pro-inflammatory adhesive receptors and coagulation-related molecules (vWF) in HUVECs[19]. However, statistical significance was not proved, and further testing will be performed.

The use of microfluidics together with the hiPSC technology brings a promising approach to *in vitro* targeting of vascular diseases. HiPSC-ECs have been reported to behave and reproduce mechanisms of primary cells, from the physiologic morphology of endothelial cells[13] and arterial phenotypic adaptations to shear[17], to the ability to form vessel-like networks[22] and present integral barrier function, with upregulation of markers of injury and inducers of inflammation[19]. Here, we conclude that they can also be used to efficiently line the walls of thrombosis-on-a-chip microfluidic devices as an *in vitro* endothelium and be tested for response to mechanisms of

thrombogenesis with comparable realism to established primary cell lines (HUVECs). Further experiments involving the use of healthy and diseased patients' hiPSC-EC and blood in thrombosis-on-a-chip setups will allow for patient-specific drug testing and the development of the personalized medicine paradigm.

Acknowledgements

I thank to those who supervised the work herein presented, namely Hugo Albers, Prof. Andries van der Meer and Prof. Cláudia Lobato da Silva. My gratitude goes also to BIOS Lab on a Chip members and director for receiving me in the laboratory.

References

1. World Health Organization. The top 10 causes of death. *Fact sheet No 310* (2017). Available at: http://www.who.int/mediacentre/factsheets/fs310/en/. (Accessed: 13th February 2018)
2. Colman, R. W. Are hemostasis and thrombosis two sides of the same coin? *J. Exp. Med.* **203,** 493–495 (2006).
3. Badimon, L., Vilahur, G. & Padro, T. Atherosclerosis and thrombosis: Insights from large animal models. *J. Biomed. Biotechnol.* **2011,** (2011).
4. Pandian, N. K. R., Mannino, R. G., Lam, W. A. & Jain, A. Thrombosis-on-a-chip: Prospective impact of microphysiological models of vascular thrombosis. *Curr. Opin. Biomed. Eng.* **5,** 29–34 (2018).
5. Westein, E., van der Meer, A. D., Kuijpers, M. J. E., Frimat, J.-P., van den Berg, A. & Heemskerk, J. W. M. Atherosclerotic geometries exacerbate pathological thrombus formation poststenosis in a von Willebrand factor-dependent manner. *Proc. Natl. Acad. Sci.* **110,** 1357–1362 (2013).
6. Costa, P. F., Albers, H. J., Linssen, J. E. A., Middelkamp, H. H. T., van der Hout, L., Passier, R., van den Berg, A., Malda, J. & van der Meer, A. D. Mimicking arterial thrombosis in a 3D-printed microfluidic in vitro vascular model based on computed tomography angiography data. *Lab Chip* **17,** 2785–2792 (2017).
7. Cao, Y., Gong, Y., Liu, L., Zhou, Y., Fang, X., Zhang, C., Li, Y. & Li, J. The use of human umbilical vein endothelial cells (HUVECs) as an in vitro model to assess the toxicity of nanoparticles to endothelium: a review. *J. Appl. Toxicol.* **37,** 1359–1369 (2017).
8. Cochrane, A., Albers, H. J., Passier, R., Mummery, C. L., Van Den Berg, A., Orlova, V. V & Van Der Meer, A. D. Advanced in vitro models of vascular biology: Human induced pluripotent stem cells and organ-on-chip technology. *Adv. Drug Deliv. Rev.* (2018). doi:10.1016/j.addr.2018.06.007
9. Passier, R., Orlova, V. & Mummery, C. Review Complex Tissue and Disease Modeling using hiPSCs. *Stem Cell* **18,** 309–321 (2016).
10. Jain, A., van der Meer, A. D., Papa, A. L., Barrile, R., Lai, A., Schlechter, B. L., Otieno, M. A., Louden, C. S., Hamilton, G. A., Michelson, A. D., Frelinger, A. L. & Ingber, D. E. Assessment of whole blood thrombosis in a microfluidic device lined by fixed human endothelium. *Biomed. Microdevices* **18,** 1–7 (2016).
11. Xia, Y. & Whitesides, G. M. Soft lithography. *Annu. Rev. Mater. Sci.* **28,** 153–184 (1998).
12. Orlova, V. V., Van Den Hil, F. E., Petrus-Reurer, S., Drabsch, Y., Ten Dijke, P. & Mummery, C. L. Generation, expansion and functional analysis of endothelial cells and pericytes derived from human pluripotent stem cells. *Nat. Protoc.* **9,** 1514–1531 (2014).
13. Belt, H., Koponen, J. K., Kekarainen, T., Puttonen, K. A., Mäkinen, P. I., Niskanen, H., Oja, J., Wirth, G., Koistinaho, J., Kaikkonen, M. U. & Ylä-Herttuala, S. Temporal Dynamics of Gene Expression During Endothelial Cell Differentiation From Human iPS Cells: A Comparison Study of Signalling Factors and Small Molecules. *Front. Cardiovasc. Med.* **5,** 1–15 (2018).
14. Barrile, R., van der Meer, A. D., Park, H., Fraser, J. P., Simic, D., Teng, F., Conegliano, D., Nguyen, J., Jain, A., Zhou, M., Karalis, K., Ingber, D. E., Hamilton, G. A. & Otieno, M. A. Organ-on-Chip Recapitulates Thrombosis Induced by an anti-CD154 Monoclonal Antibody: Translational Potential of Advanced Microengineered Systems. *Clin. Pharmacol. Ther.* **00,** 1–9 (2018).
15. Silva Simão, J. P. Implementation of hiPSC-ECs in thrombosis-on-a-chip devices. (Instituto Superior Técnico, University of Lisbon, 2018).
16. Sivarapatna, A., Ghaedi, M., Xiao, Y., Han, E., Aryal, B., Zhou, J., Fernandez-Hernando, C., Qyang, Y., Hirschi, K. K. & Niklason, L. E. Engineered Microvasculature in PDMS Networks Using Endothelial Cells Derived from Human Induced Pluripotent Stem Cells. *Cell Transplant.* **26,** 1365–1379 (2017).
17. Smith, Q., Macklin, B., Chan, X. Y., Jones, H., Trempel, M., Yoder, M. C. & Gerecht, S. Differential HDAC6 Activity Modulates Ciliogenesis and Subsequent Mechanosensing of Endothelial Cells Derived from Pluripotent Stem Cells. *Cell Rep.* **24,** 895–908.e6 (2018).
18. Sivarapatna, A., Ghaedi, M., Le, A. V, Mendez, J. J., Qyang, Y. & Niklason, L. E. Arterial specification of endothelial cells derived from human induced pluripotent stem cells in a biomimetic flow bioreactor. *Biomaterials* **53,** 621–33 (2015).
19. Halaidych, O. V., Freund, C., van den Hil, F., Salvatori, D. C. F., Riminucci, M., Mummery, C. L. & Orlova, V. V. Inflammatory Responses and Barrier Function of Endothelial Cells Derived from Human Induced Pluripotent Stem Cells. *Stem Cell Reports* **10,** 1642–1656 (2018).
20. Cooley, B. C. In vivo fluorescence imaging of large-vessel thrombosis in mice. *Arterioscler. Thromb. Vasc. Biol.* **31,** 1351–6 (2011).
21. Gale, A. J. Continuing Education Course #2: Current Understanding of Hemostasis. *Toxicol. Pathol.* **39,** 273–280 (2011).
22. Bezenah, J. R., Kong, Y. P. & Putnam, A. J. Evaluating the potential of endothelial cells derived from human induced pluripotent stem cells to form microvascular networks in 3D cultures. *Sci. Rep.* **8,** 1–10 (2018).